



# Structural, Optical and Sensing Behavior of Neodymium-Doped Vanadium Pentoxide Thin Films

Iftikhar M. Ali<sup>1</sup> · Jamal M. Rzaij<sup>2</sup> · Qayes A. Abbas<sup>3</sup> · Isam M. Ibrahim<sup>1</sup> · Hassan J. Alatta<sup>4</sup>

Received: 9 December 2016 / Accepted: 2 April 2018 / Published online: 1 August 2018  
© Shiraz University 2018

## Abstract

In this study, nanocrystals of vanadium pentoxide ( $V_2O_5$ ) thin films were manufactured by chemical spray pyrolysis technique. A precursor solution of 0.05 M  $VCl_5$  was prepared using distilled water. Neodymium (Nd)-doped vanadium oxide films were fabricated, increasing the neodymium chloride by ratios of 0, 3, 5, 7 and 9% in separate solutions. These precursor solutions have been utilized to grow films of undoped  $V_2O_5$  and doped with Nd on the p-type Si (111) porous silicon (PS) and glass substrates at temperatures of 250 °C. The structural, optical, electrical and gas sensing properties were studied. The analysis of the structural and optical properties of the thin films shows the effect of doping rates on the characteristics of vanadium oxide. The X-ray diffraction investigation resulted in a polycrystalline nature of the orthorhombic structure with the preferred direction of (010) with nano-grain sizes. Atomic force microscopy (AFM) was used to characterize the morphological properties of the films. Undoped  $V_2O_5$  and doped  $V_2O_5$  with various concentrations of Nd films directly allowed the transition of the band gap. The sensitivity of  $NO_2$  and  $H_2$  gases for various doping ratios of Nd at different operating temperatures was measured.

**Keywords** Vanadium oxide · Structural properties · Electrical properties · Sensing behavior

## 1 Introduction

Recent developments in nanotechnology have heightened the need to find new materials to use in sensors. The metal oxide is presently considered to be one of the most suitable groups to use for applications such as gas sensors (Fine et al. 2010). Semiconductor metal oxides have been used in many applications and are still in persistent development. Thin films are one of the good techniques that share in the evolution of semiconductor technology. (Phanichphant 2014). Vanadium oxide is of significant research importance owing to its multivalent behavior. The vanadium oxides occur in the oxidation states such as  $V^{2+}$ ,  $V^{3+}$ ,  $V^{4+}$  and  $V^{5+}$  as well as in the form of materials such as VO,  $V_2O_3$ ,  $VO_2$  and  $V_2O_5$  (Margoni et al. 2015). Accordingly, vanadium pentoxide ( $V_2O_5$ ) has considerable potential in plentiful applications owing to its significant properties such as polyvalency, layered structure, stability both chemically and thermally, and good thermoelectric effect; thus these characteristics have made vanadium pentoxide ( $V_2O_5$ ) a favorable material for applications in electronics, and in both electrochemical and optoelectronic

✉ Iftikhar M. Ali  
iftikhariq@gmail.com

Jamal M. Rzaij  
jam72al@gmail.com

Qayes A. Abbas  
qaaal-dulaim1@sheffield.ac.uk

Isam M. Ibrahim  
dr.issamiq@gmail.com

Hassan J. Alatta  
hassan.jaber2020@gmail.com

<sup>1</sup> Department of Physics, College of Science, University of Baghdad, Baghdad, Iraq

<sup>2</sup> Department of Physics, College of Science, University of Anbar, Ramadi, Iraq

<sup>3</sup> Department of Physics, College of Education for Pure Science, University of Anbar, Ramadi, Iraq

<sup>4</sup> Department of Scientific Affaires, University of Baghdad, Baghdad, Iraq

systems. Previous studies have reported that vanadium pentoxide can be utilized as a catalyst, gas sensor, and also as electronic and optical switching devices (Benmoussa et al. 2002). Different chemical and physical mechanisms such as spray pyrolysis (Mousavi and Kompany 2012; Mrigal et al. 2015; Vijayakumar et al. 2015), electron beam evaporation (Shrividhya et al. 2015), thermal evaporation (Tashtoush and Kasasbeh 2013), pulsed laser deposition (Beke et al. 2009), and sol–gel (Alamarguy et al. 2006) have been used to prepare the vanadium pentoxide thin films. The structural, optical and electrical properties of vanadium pentoxide films have been investigated in several studies. Examples include a study of structural and semi-conducting properties of non-crystalline vanadium pentoxide manufactured by splat cooling by Rivoalen et al. (1976). In another study, the structural and optical investigations for  $V_2O_5$  thin films showed two electrochromic steps, yellow to green and then green to blue (Benmoussa et al. 2002). Pan et al. (2010) suggested a technique of a superficial synthesis for manufacturing nanosized  $V_2O_5$  by utilizing vanadyl oxalate in atmosphere for high-rate lithium batteries. The current work is focused on studying the effect of doping ratios of neodymium on the structural, optical and sensing performance of the semiconducting  $V_2O_5$  thin films prepared by (CSPT) with the main aim of improving the sensitivity of these films as a gas sensor for  $NO_2$  and  $H_2$  gases.

## 2 Experimental Procedure

In this work,  $V_2O_5$  thin films were prepared on glass and single-crystal silicon wafer *p*-type (111) substrates using spray pyrolysis technique. The spray pyrolysis apparatus used in this work consists of a homemade spraying unit, a substrate holder with heater, and an enclosure. The glass substrate is kept on a stainless steel plate. The conditions of preparation are as follows: nozzle-substrate distance is 30 cm, gas pressure is 3 bar and spray time is 5 s with stopping time of 10 s at 325 °C substrate temperature with  $O_2$  carrier gas at 3 ml/min solution flow rate. The structural aspects were investigated by X-ray diffraction (PW1840) using Cu  $K_\alpha$  radiation. Optical transmission for samples was measured with a UV–visible spectrophotometer Cary 100 in the range 300–900 nm. Aqueous solutions of 0.05 M of ( $VCl_5$ ) with purity 99.8% from BDH chemical Ltd pool England and 0.05 M of ( $NdCl_3$ ) of purity 99.9% provided from Flukea Swesria company. These solutions were prepared from dissolving them in 100 ml of distilled water. These two solutions are mixed by magnetic stirrer for 1 h at 60 °C to ensure that Nd atoms are well distributed in vanadium host material, then an appropriate volume for each experiment is taken depending on the

volume percentage of addition where (Nd:V = 0, 3, 5, 7, 9%).

After cleaning the substrates, they were placed on the flat plate heater surface, which is electrically controlled, and left for about 10 min to allow their temperature to reach the set temperature at  $(250 \pm 5)$  °C. Then the solution must be put in sprayer container. After that, the deposition process starts within deposition time of 5 s, then stopped this process for 10 s; when the fine droplets arrive at the substrate, the solid compounds react to become a new chemical compound. The atomization of the solution into a spray of fine droplets is carried out by the spray nozzle, with the help of compressed oxygen ( $O_2$ ) as carrier gas. After the spray process is completed, then the hot plate will be shut down and the samples are left on the surface of the heater to reach the room temperatures, then the substrates can be raised. Finally, the structural, optical and electrical properties for films were characterized.

The X-ray diffraction (XRD) spectra of the films were acquired to investigate their crystal structure using a (Cu- $K_\alpha$ ) radiation with  $\lambda = 0.154$  nm. Optical transmission data were obtained using UV–Vis double beam spectrometer at wavelengths ranging from 200 to 900 nm. Atomic force microscopy (AFM) was utilized to study the surface morphology of the films.

## 3 Results and Discussion

### 3.1 Structural Properties

The results of X-ray diffraction, as shown in Fig. 1, indicate that for the undoped and doped  $V_2O_5$  with 3, 5, 7 and 9% concentrations of Nd there is a high intensity and sharp peak at  $2\theta = 28^\circ$ , it is attributed to the crystalline Si substrate with crystalline plane (111). The acquired XRD patterns have polycrystalline vanadium pentoxide structure with planes (200), (010), (110), (101), (400), (301), (600) and (002) which is in agreement with previous studies (Kaid 2006; Johansson 2011). Crystallization of the films were in the orthorhombic phase as stated by International Centre for Diffraction (ICDD PDF No. 96-101-1226), which match those observed in previous studies (Margoni et al. 2015; Chakrabarti et al. 1999; Shevchuk et al. 2011; Josephine et al. 2015). It is observed that the preferred orientation of the film is along the (010) plane with a diffraction angle of  $2\theta = 20.36^\circ$ ,  $d = 4.35$  nm and in addition, it found that the lattice parameter values obtained were  $a = 11.4734$  Å,  $b = 4.35809$  Å and  $c = 3.5533$  Å, which are similar to results obtained in (Chakrabarti et al. 1999; Hermann et al. 1999). The average crystallite size was found to be equal to 26.29 nm. It was calculated using the Debye–Scherrer's formula (shown below) for the (010) reflection.

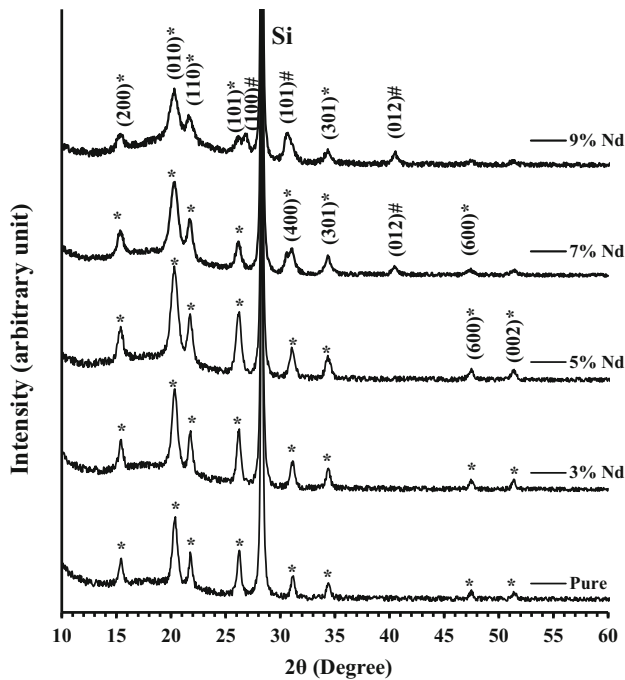


**Fig. 1** The XRD results of Nd-doped V<sub>2</sub>O<sub>5</sub> thin films. Asterisk is denoted to V<sub>2</sub>O<sub>5</sub> and hash is denoted to Nd<sub>2</sub>O<sub>3</sub>

$$D = \frac{0.94\lambda}{\beta \cos\theta} \tag{1}$$

where  $\lambda$  is the wavelength of XRD photons which equal to 0.154 nm,  $\beta$  is the full-width at half maximum (FWHM) and  $\theta$  is the Bragg diffraction angle in degrees.

At the doping ratios of 3 and 5% Nd, there was a significant increase in the intensity of the diffraction, due to the absence of new peaks for the doping material, (neodymium oxide), in the XRD pattern of these ratios. While at the concentrations 7 and 9%, it was observed that there was a reduction in the proportion of intensity for the vanadium pentoxide reflection peaks caused by the occurrence of new crystalline planes coming from the structure of doping material, which have low intensities comparing with intensities of V<sub>2</sub>O<sub>5</sub> peaks, the peaks are: (100), (101) and (012) at diffraction angles ( $2\theta$ ) equal to 26.85°, 30.59° and 40.48°, respectively, which belong to Nd<sub>2</sub>O<sub>3</sub> and have a cubic phase structure, as stated by the (ICDPDF No.96-

200-2850). From the result of the XRD, it is observed that the direction of crystalline growth is not changed by the ratios of doping for the dominant planes, the growth continues in the direction (010) referring to the model of the drift competitive growth, which is known as “the model of the survival of the fastest growing crystallites” (van der Drift 1967). From the XRD pattern, it is found that the full width at half maximum (FWHM) increased and this leads to a reduction in the size of crystals as the doping ratio for Nd increases compared to pure vanadium pentoxide films using the Scherrer’s formula shown in Eq. (1). The decrease of the crystallite due to doping way is proof of the improvement of the nanocrystalline size. Using both the equations of Scherrer and Williamson–Hall, the average crystal size ( $D_{ave}$ ) has been calculated. The two methods produced similar results and the difference in the values of the crystallite size is small as shown in Table 1.

The lattice constants ( $a$ ,  $b$ , and  $c$ ) of undoped V<sub>2</sub>O<sub>5</sub> and doped thin films of various ratios were computed for the planes (200), (010) and (101), which are recorded in Table 2. It can be seen that there is an increase in the lattice constant as the ratio of doping increases, this can be attributed to the doping with Nd which influences the structure of the crystalline V<sub>2</sub>O<sub>5</sub> thin films. It could also be due to the increase of oxygen vacancies through the doping method.

### 3.2 Atomic Force Microscopy (AFM) Analysis

AFM pictures in three dimensions and the grain density distribution chart of both pure and doped V<sub>2</sub>O<sub>5</sub> thin films for various doping ratios of 0, 3, 5, 7 and 9% grown on glass substrates are illustrated in Fig. 2. A higher surface

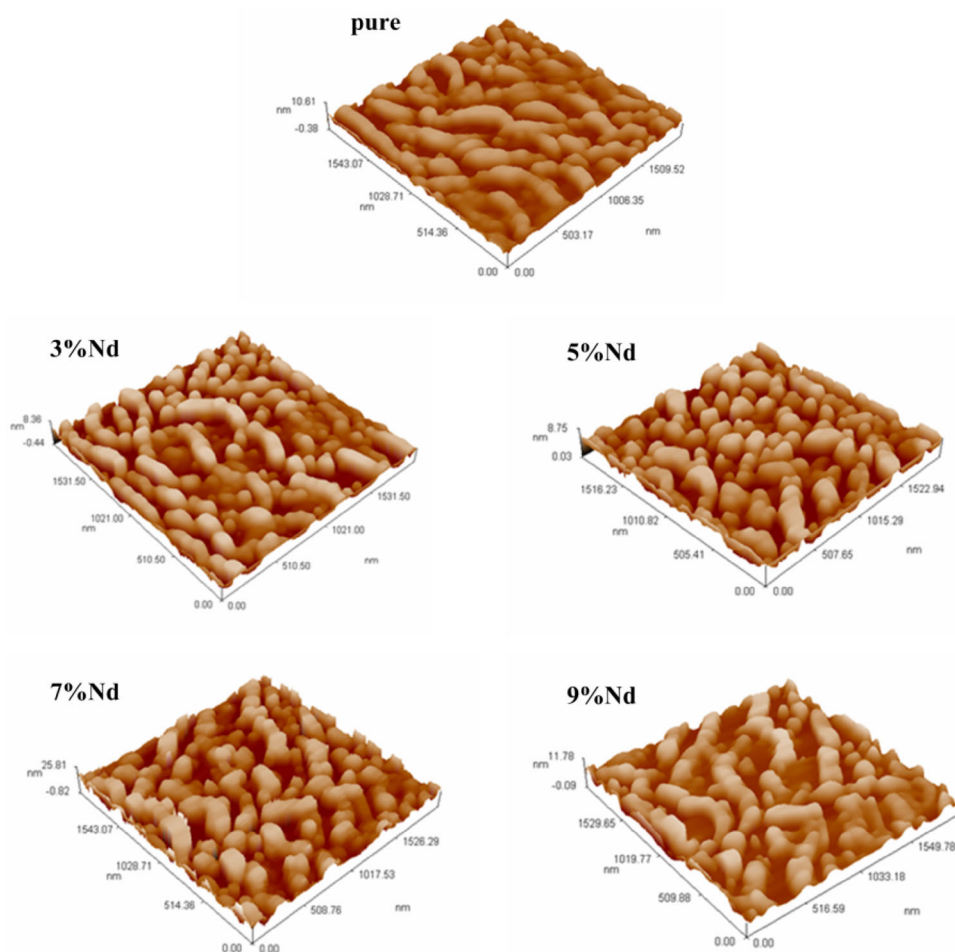
**Table 1** Crystalline size and strain extracted from Scherer’s formula and Williamson–Hall relations for pure and doped V<sub>2</sub>O<sub>5</sub> films

Doping ratio (%)	$D_{ave}$ (Sh) nm	$D_{ave}$ (W) nm	Strain
0	26.29	20.69	0.0015
3	23.31	19.25	0.0011
5	17.81	14.45	0.0014
7	16.11	11.75	0.0032
9	15.49	9.97	0.005

**Table 2** Lattice parameters for pure and doped films

Nd%	L.C					
	$a$ (Å) EXP.	$\Delta a/a_0$	$b$ (Å) EXP.	$\Delta b/b_0$	$c$ (Å) EXP.	$\Delta c/c_0$
0	11.473	0.00061	4.358	0.000459	3.553	0.000563
3	11.489	0.000784	4.362	0.000459	3.556	0.000281
5	11.506	0.002265	4.367	0.001606	3.558	0.000844
7	11.521	0.003571	4.371	0.002523	3.561	0.001688
9	11.537	0.004965	4.376	0.00367	3.563	0.00225

**Fig. 2** AFM pictures and size distributions of  $V_2O_5$  thin films with different doping ratios of Nd



area was achieved in the granular films, which is useful for film–gas influence as it has a higher sensitivity, due to the relation between the film roughness and the gas sensitivity. Morphological properties such as the average diameter, average roughness, average r.m.s roughness and peak–peak for films are presented in Table 3.

The analysis of AFM images shows that the film for undoped  $V_2O_5$  has much bigger likeness strip-shape grain created. Besides that, it has a good uniformity revealing a regular growth of the films. The increase in the doping ratios with Nd decreases the grain size, which is calculated from acquired from X-ray results. For the doped films, the roughness average increased, with grains randomly

distributed for the doping concentrations of 3 and 5%. However, a doping ratio of over 5% causes the roughness average to decrease.

## 4 Optical Properties

### 4.1 Transmittance (T)

Figure 3 illustrates the change of the optical transmission of pure  $V_2O_5$  and doped with 3, 5, 7 and 9% of Nd thin films, which are sprayed on the glass substrate, as a function of the wavelength from 300 to 900 nm. An increase in

**Table 3** Morphological properties for pure  $V_2O_5$  and doped with several concentrations of Nd

Sample	Average grain size (nm)	Average roughness (nm)	r.m.s roughness (nm)	Peak–peak (nm)
0% Nd	127.91	1.5	1.98	19
3% Nd	122.1	2.43	2.82	13.1
5% Nd	96.27	2.65	3.02	14
7% Nd	91.69	1.45	1.67	7.16
9% Nd	87	1.43	1.64	7.41

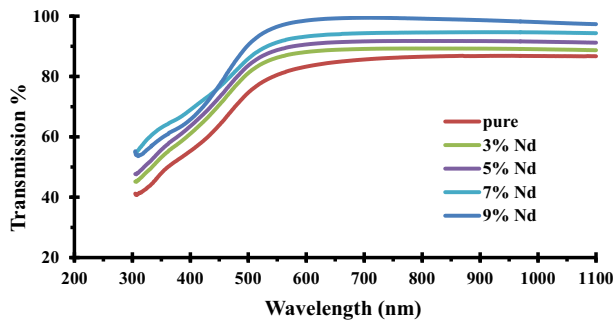


**Fig. 3** Transmission against the wavelength for pure  $V_2O_5$  and doped with Nd at several doping ratios

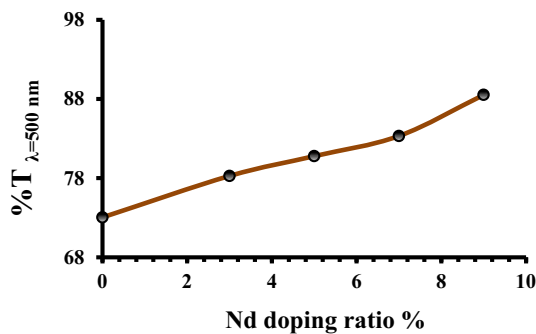


**Fig. 4**  $T_{\lambda=500 \text{ nm}}$  % against doping ratios for pure  $V_2O_5$  and doped samples

the wavelength increased the transmission to the maximum value of 79%, which is in agreement with the findings in (Prameela et al. 2013; Sieradzka 2011; Prociow et al. 2011). As a result, the increase of the transmission with an increase in the doping ratio of Nd is due to the reduction in the absorption in the visible region. It is observed that all the films show a transmission above (79%) in the visible range with an acute absorption edge.

Figure 4 shows the alteration of transmission at the wavelength of ( $\lambda = 500 \text{ nm}$ ) as a function of the doping percentages which exhibits an increase in transmission with increasing of the doping ratio. All the films show an elevated transparency in the visible region. This is due to the weak absorption in the films (Kaid 2006), meaning that the films are appropriate for use as a window gap solar cells in view of the fact that the active spectral region in solar cells exists in the visible spectrum.

## 4.2 Optical Energy Gap ( $E_g$ )

Optical energy gap for  $V_2O_5$  films grown on glass substrates at  $T_s$  equal to  $250^\circ\text{C}$  in various doping concentrations of 3, 5, 7, and 9% was achieved in the range (300–900) nm of wavelength by extrapolating from the linear portion of the plot  $(\alpha h\nu)^2$  against  $(h\nu)$  for zero absorption coefficient value as shown in Fig. 5, and it can

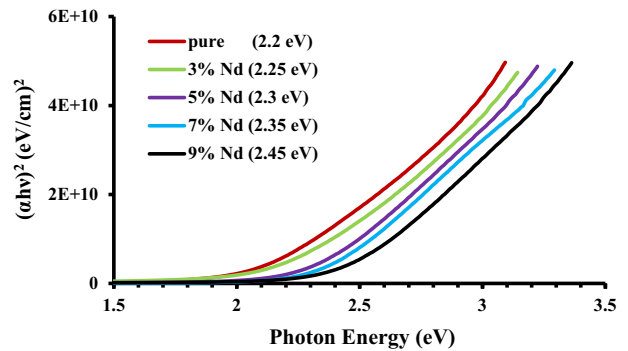


**Fig. 5** Tauc plot for pure  $V_2O_5$  and doped with Nd at various doping ratios

be seen that the un-doped  $V_2O_5$  and doped films possess a direct transition band gap of about 2.2 eV. This outcome is sensible and closer to other ( $E_g$ ) values investigated in previous studies (Vijayakumar et al. 2015; Tashtoush and Kasasbeh 2013; Aquino-Meneses et al. 2014; Benmoussa et al. 2003).

We observed a slight increase in  $E_g^{\text{opt}}$  with a change in the concentration of the films. This is attributed to the influence of disorder, defects, and impurity in the structure of the semiconductors causing the inner electric fields to affect the band tails close to the edge (Ozutok et al. 2012). From the result of optical energy gap, it is found that all the films possess localized states which produce from the intensity of defects at the boundaries of grains as well as the donor levels, and it can be deduced that by controlling impurity rate and the size of nanocrystal the optical energy gap can be changed.

## 4.3 Gas Sensing Measurement

In this work, the temperature dependence of the sensitivity of two different gases ( $\text{NO}_2$  and  $\text{H}_2$  gases) have been used to study the sensing properties of undoped  $V_2O_5$  and doped with various concentrations of Nd films grown on porous silicon substrates at 20 min and etching current of 20 mA, by changing the operating temperature and time.

## 5 Measurement for $\text{NO}_2$ Gas

### 5.1 Sensing Performance of $V_2O_5$ :Nd Films for $\text{NO}_2$ gas

The prepared samples have been tested for gas sensing properties using  $\text{NO}_2$  gas with a concentration of 25 ppm at various operating temperatures starting from room temperature to  $200^\circ\text{C}$  with steps of  $50^\circ\text{C}$ . The change in resistance (R) with the time during on/off gas valve state can be seen in Fig. 6a–e. The ionosorption of gas species is

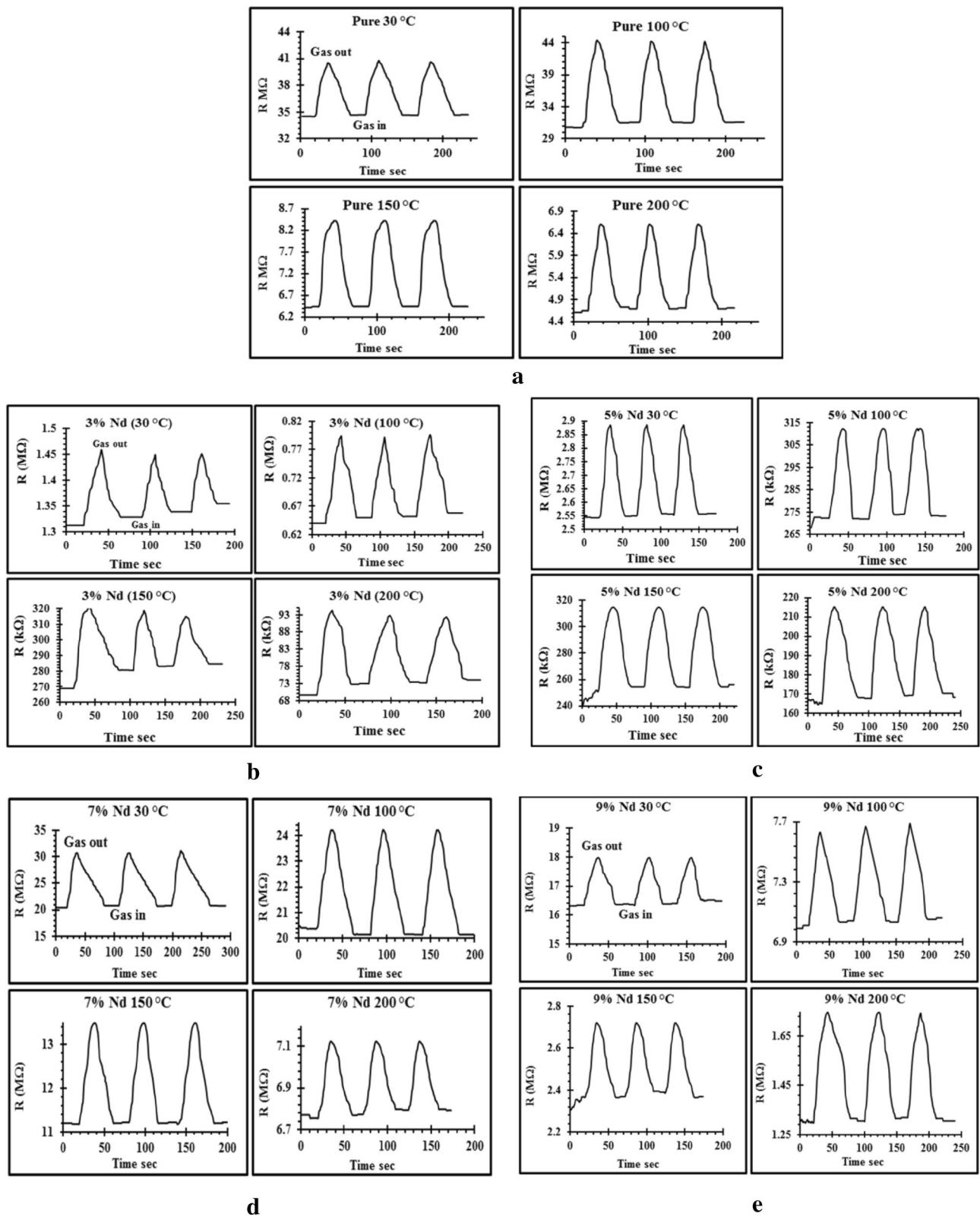
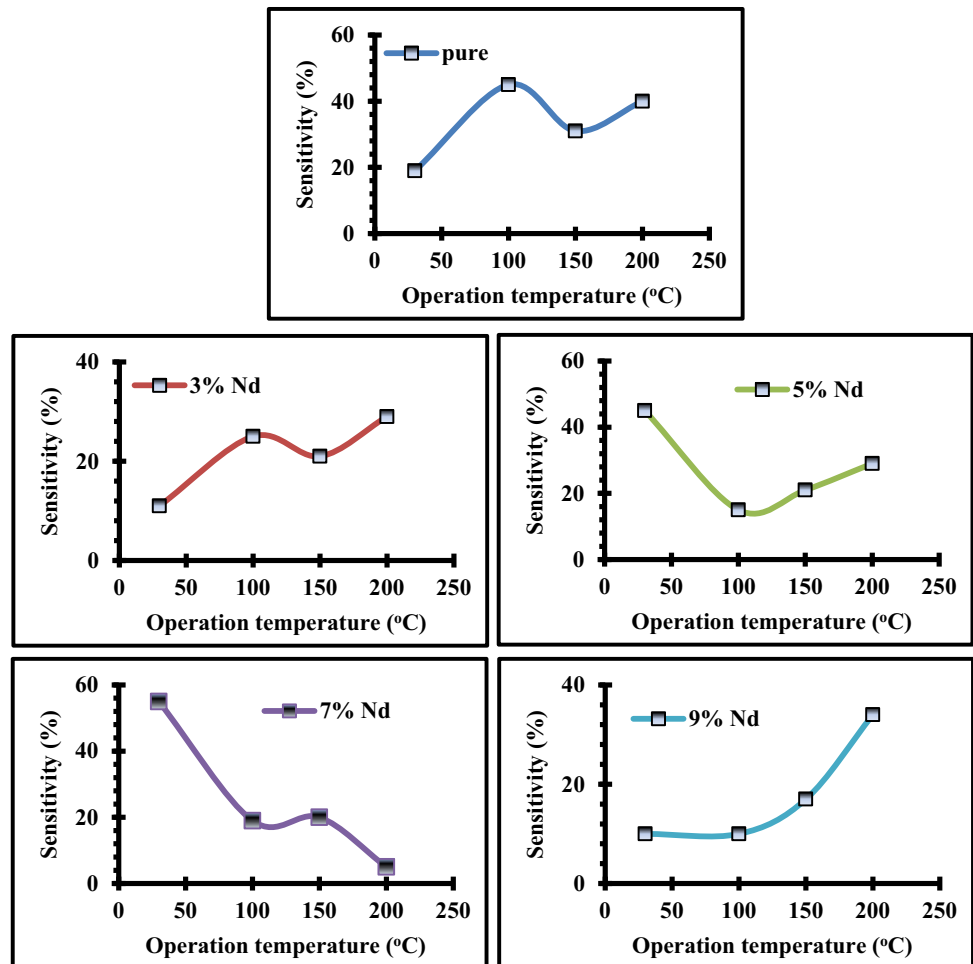


**Fig. 6** The difference of resistance with time for  $\text{NO}_2$  gas **a** pure films, **b** 3% Nd, **c** 5% Nd, **d** 7% Nd and **e** 9% Nd

**Fig. 7** The difference of NO<sub>2</sub> sensitivity with operating temperature of the pure V<sub>2</sub>O<sub>5</sub> and doped thin films



connected to the sensing properties of V<sub>2</sub>O<sub>5</sub> films, which is due to the charge transfer between the gas and surface molecules leading to an effect on the electrical conductivity (Filipovic et al. 2013). These figures showed that the resistance values increased when the films were exposed to NO<sub>2</sub> gas, (Gas ON), while during the closure of the gas (Gas OFF) the resistance values decreased. This behavior is due to the NO<sub>2</sub> gas undergoing an ionic reaction with the surface adsorption oxygen, where the electron on the oxygen is removed from the semiconductors which then decreases the conductance of V<sub>2</sub>O<sub>5</sub> films thus leading to an increase in their resistivity (Wang et al. 2010).

The change in values of resistance of the semiconductor sensors depends on the atmosphere in which it is placed. In air, oxygen is adsorbed on the surface and dissociates leading to the formation of O<sup>-</sup> and in this case the electron on the oxygen is extracted from the metal oxide semiconductor. This extracted electron tends to enhance the resistance of n-type semiconductors which have an abundance of electrons as the majority charge carriers. In the presence of gases, such as the nitrogen and NO<sub>2</sub>, the nitrogen reacts

with the adsorbed O<sup>-</sup> to form NO<sub>2</sub> and the electron is re-injected inside the semiconductor films, where it causes the resistance to decrease (Iftikhar and Massar 2017). The sensitivity factor (*S*%) for different operating temperatures is measured using the formula:

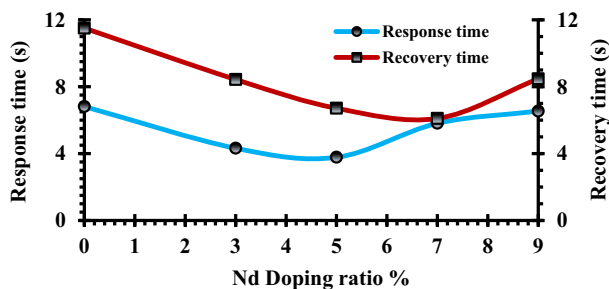
$$S = \left| \frac{R_g - R_a}{R_a} \right| \times 100\% \quad (2)$$

where *S* is the sensitivity, *R<sub>a</sub>* and *R<sub>g</sub>* are the electrical resistance of the film in the air and electrical resistance of the film in the presence of gas, respectively. Figure 7 shows the change of the sensitivity with the change of the operating temperatures for undoped V<sub>2</sub>O<sub>5</sub> and doped with various concentrations of Nd, which are grown on the PS substrates. The gas sensitivity tests were carried out at room temperature (30 °C) and reached to 200 °C by 50 °C steps.

The results indicate that the sensitivity of the films increase with an increase of the operating temperature. It is evident from the figures that the sensitivity of the films can gradually increase during the increase of the operating

**Table 4** Sensitivity % of pure  $V_2O_5$  and doped with altered ratios of Nd for  $NO_2$  gas

%Nd	Sensitivity % at				Response time (s) at				Recovery time (s) at			
	RT	100 °C	150 °C	200 °C	RT	100 °C	150 °C	200 °C	RT	100 °C	150 °C	200 °C
0	19	45	31	40	6.81	5.65	5.89	6.56	11.5	9.07	7.7	8.23
3	11	25	18	37	4.32	7.24	5.73	8.14	8.43	9.52	15.36	7.11
5	45	15	21	29	3.78	5.18	5.91	7.3	6.71	3.67	7.55	13.14
7	55	19	20	5	5.81	5.66	5.5	3.5	6.1	9.19	7.78	8.16
9	10	10	17	34	6.54	6.76	3.9	6.98	8.47	10.98	8.03	12.61

**Fig. 8** The difference of response time and recovery time with Nd doping ratios at room temperature

temperature. That can be attributed to the enhancement in the rate of surface reaction of the gas. It is also important to note that there is a decrease in the sensitivity of the 7% Nd-doped film during the increase of the operating temperature. This could be due to the surface being incapable of oxidizing the gas and the higher temperature could then lead to the burning of the  $NO_2$  gas before arriving at the surface of the films. Consequently, the gas sensitivity can be decreased with increasing the temperature (Garde 2010). It can be observed that the maximum value of sensitivity to  $NO_2$  gas was in the film doped with 7% Nd and was found to be 55% at RT. This doping ratio shifted the operating temperature to RT with the highest sensitivity thus the sensor has a sensitivity to  $NO_2$  gas in the absence of heating the sensor which is more practical to use as shown in Table 4.

Figure 8 illustrates both the response time and the recovery time with altered neodymium oxide-doping ratios at optimal operating temperature of the  $V_2O_5$  thin films.

The response speed has been studied at the temperature in which the sensor shows a maximum sensitivity. The above figure illustrates that the 7% Nd-doped specimens show a rapid response speed (5.81 s) with recovery time (6.1 s), meaning that a small magnitude of impurities is the best doping ratio to achieve rapid response of the sensor. The rapid response of the sensor for  $NO_2$  gas perhaps is due to a quicker oxidation of the gas (Garde 2010). Additionally, it can be due to the increase of vacancies in oxygen

produced in the  $V_2O_5$ :Nd lattice. On the other hand, neodymium ions take the energy level under the conduction band and possess an activator behavior, allowing the electrons to move easily to conduction band, which leads to the formation of an electron-depleted surface layer due to an increase in the adsorbed oxygen on the surface then removes the conduction electrons from the near surface region. This will in turn increase the number of effective adsorption locations, thus attaining rapid response time for the sensor (Sujitno and Sudjatmoko 2011). In real conditions, the measurements of sensitivity generally require a rapid response time, while a quick recovery time is not very important.

## 6 Measurement of $H_2$ Gas

### 6.1 Sensing Performance of $V_2O_5$ :Nd Films for $H_2$ Gas

Figure 9a–e illustrates the sensing properties and the difference of resistance versus the time. It can be seen that the exposure of the films to  $H_2$  gas causes a decrease in the resistance which further decreases at the closing of the gas. The possible mechanism for that is due to the reaction between hydrogen and the chemisorbed oxygen on the surface which can cause the difference in the surface electron depletion area (Isam et al. 2015).

The sensitivity factor ( $S\%$ ) at different operating temperatures is presented in Fig. 10. The sensitivity of all films changed increasingly with increase of the operating temperature. It is clear from the result of sensitivity, that an increase in the operating temperature enhances the sensitivity of the films due to an increase in the ratio of surface reaction of the used gas, excluding the films doped with 3 and 5% of Nd which showed a decrease in their sensitivity with an increase of the operating temperature to 200 °C, but after this temperature the sensitivity increasingly changed. The cause for this perhaps comes from the surface that would be incapable of oxidizing the gas intensely and



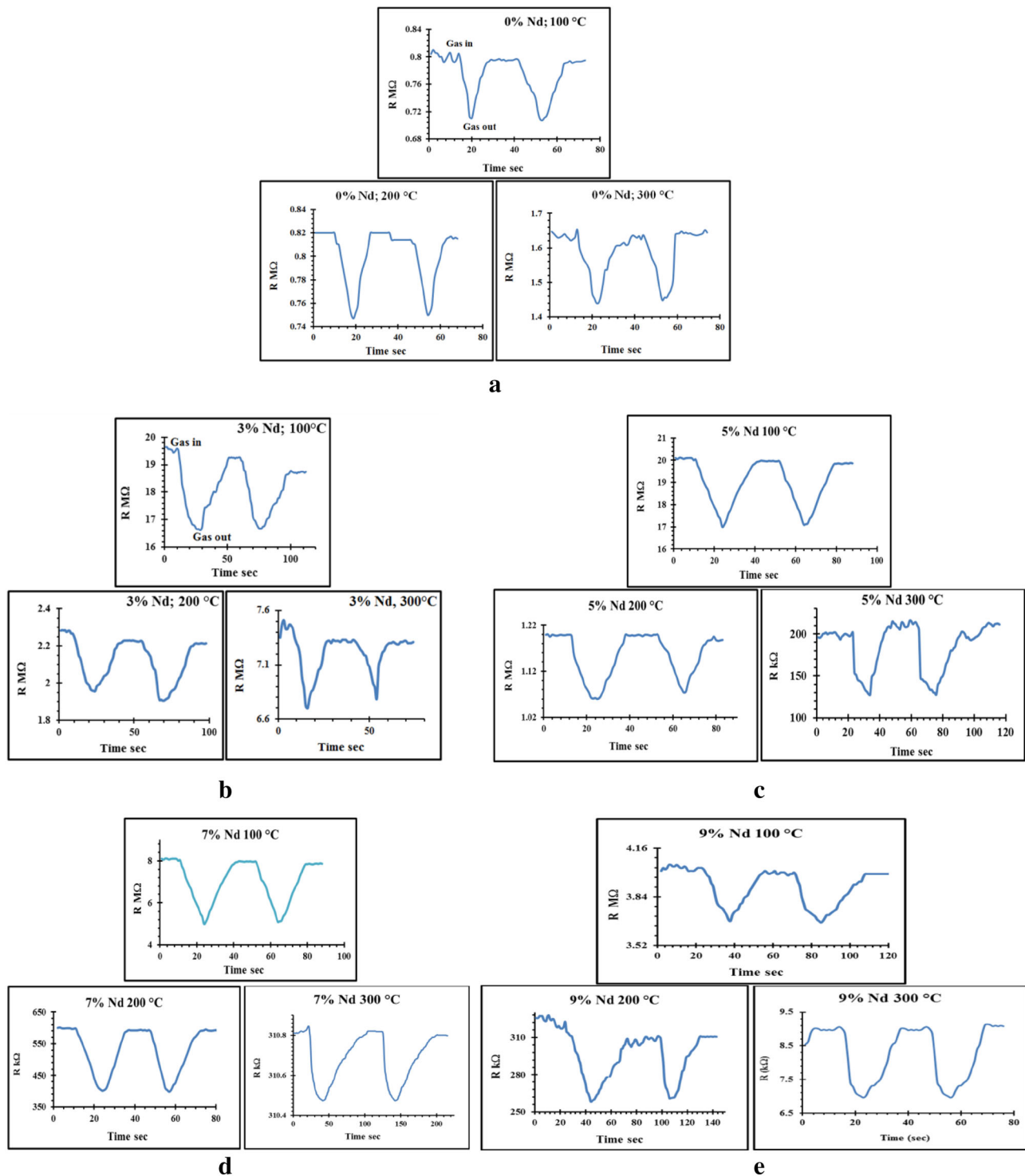


**Fig. 9** The difference of resistance against the time as H<sub>2</sub> gas **a** pure films, **b** 3% Nd, **c** 5% Nd, **d** 7% Nd and **e** 9% Nd

the H<sub>2</sub> gas perhaps burning before arriving at the surface of the film at identifying temperature. This leads to a decrease in the gas sensitivity (Garde 2010).

It was observed that the temperature of 300 °C was the optimal temperature and the higher sensitivity of H<sub>2</sub> gas was found in the film doped with 7% Nd and it is equal to

60%, as shown in Fig. 11, rapid response and recovery time are shown in Fig. 12, and the results are recorded in Table 5.

**Fig. 10** The difference of sensitivity against the operating temperature of the  $V_2O_5$  thin films for  $H_2$

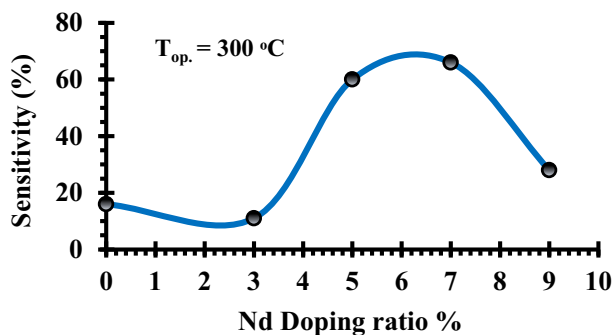
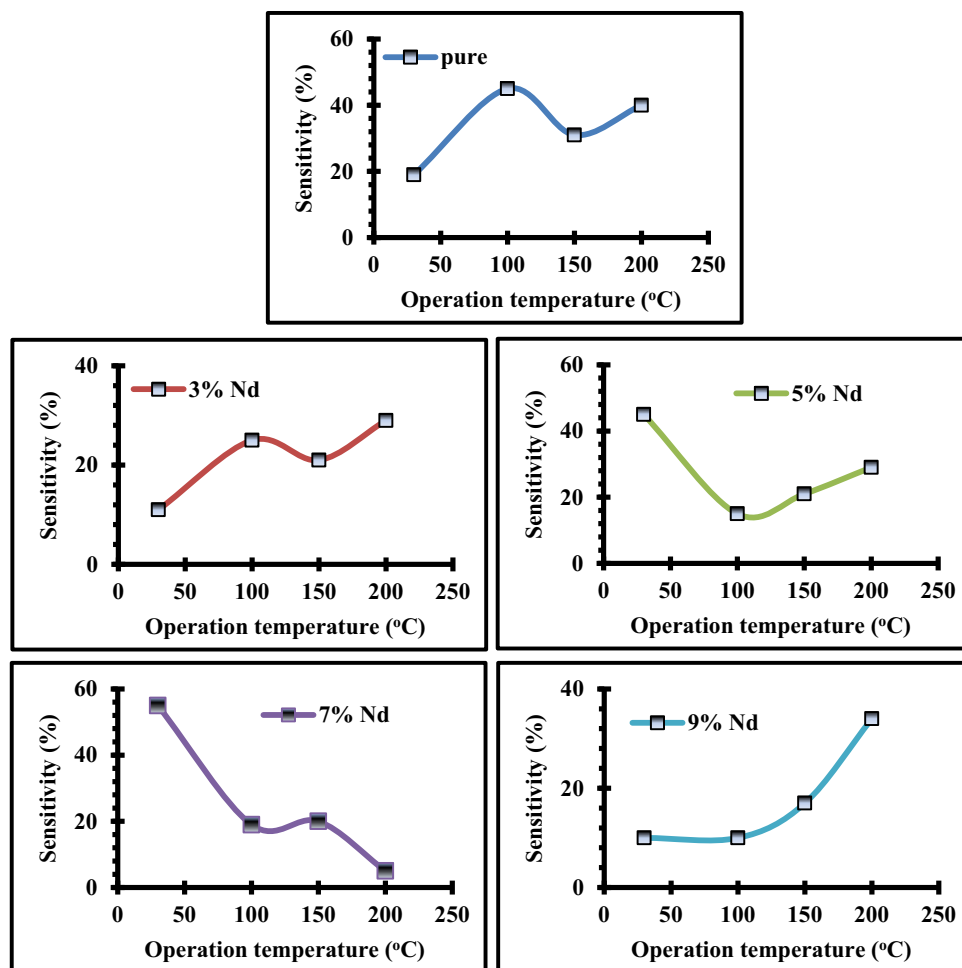


**Fig. 11** The change of  $H_2$  sensitivity versus the operating temperature at  $300^\circ C$  of the  $V_2O_5$  thin films

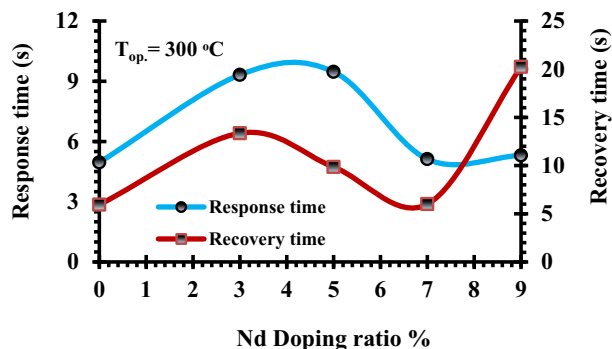


**Fig. 12** The change of response time and recovery time versus Nd-doping ratios at  $300^\circ C$  operating temperature

## 7 Conclusion

In this study, pure vanadium pentoxide and Nd doped with various concentrations (3, 5, 7 and 9)% were deposited on a glass slide, Si (111) *p*-type and PS substrates by spray pyrolysis technique at  $250^\circ C$  substrate temperature. XRD results presented polycrystalline structure in orthorhombic phase and favoured an orientation of (010). The

transmission of undoped  $V_2O_5$  attained the maximum value of about 79% and it also increased with an increase in Nd-doping ratio. As the Nd concentration increased, the optical energy gap increased from 2.2 eV to 2.4 with increasing of Nd concentration. The maximum sensitivity to  $NO_2$  gas occurred in the film doped with 7% Nd and was determined to be 55% at room temperature whilst the maximum sensitivity to  $H_2$  gas was observed in the sample doped with

**Table 5** Sensitivity %, response and recovery times of V<sub>2</sub>O<sub>5</sub> thin films for H<sub>2</sub> gas

%Nd	Sensitivity % at			Response time (s) at			Recovery time (s) at		
	100 °C	200 °C	300 °C	100 °C	200 °C	300 °C	100 °C	200 °C	300 °C
0	10	12	16	8.444	5.8	4.96	5.75	9.1	5.95
3	18	17	11	9.83	4.9	9.32	18.89	9.68	13.36
5	17	13	60	9.63	9.86	9.47	12.2	14.12	9.85
7	33	50	66	9.63	6.07	5.12	12.12	7.777	6
9	9	19	28	9.85	8	5.31	14.02	14.17	20.24

7% Nd and was determined to be 66% at 300 °C with small response and recovery times.

**Acknowledgements** The authors acknowledge the University of Baghdad, College of Science, Department of Physics, for support to this research and Dr. Precious Shamba for her help.

## References

- Alamarguy D, Castle JE, Ibris N, Salvi AM (2006) Characterisation of sol gel crystalline V<sub>2</sub>O<sub>5</sub> thin films after Li intercalation cycling. *Surf Interface Anal* 38(4):801–804
- Aquino-Meneses L, Lozada-Morales R, del Angel-Vicente P, Percino-Picazo JC, Zelaya-Angel O, Becerril M, Carmona-Rodríguez J, Rodríguez-Melgarejo F, Jiménez-Sandoval S (2014) Photoluminescence in Nd-doped V<sub>2</sub>O<sub>5</sub>. *J Mater Sci* 5(3):2298–2302
- Beke S, Korsi L, Papp S, Oszk A, Nnai L (2009) XRD and XPS analysis of laser treated vanadium oxide thin films. *APSUSC Appl Surf Sci* 255(24):9779–9782
- Benmoussa M, Outzourhit A, Bennouna A, Ameziane E (2002) Electrochromism in sputtered V<sub>2</sub>O<sub>5</sub> thin films: structural and optical studies. *Thin Solid Films* 405(1–2):11–16
- Benmoussa M, Outzourhit A, Jourdani R, Bennouna A (2003) Structural, optical and electrochromic properties of sol–gel V<sub>2</sub>O<sub>5</sub> thin films. *Act Passiv Electron Compon* 26(4):245–256
- Chakrabarti A, Hermann K, Druzinic R (1999) Geometric and electronic structure of vanadium pentoxide: a density functional bulk and surface study. *Phys Rev B* 59(16):583–590
- Filipovic L, Selberherr S, Mutinati GC, Brunet E, Steinhauer S, Anton K, Teva J, Kraft J, Schrank F, Gspan C, Grogger W (2013) A method for simulating spray pyrolysis deposition in the level set framework. *Eng Lett* 21(4):224–240
- Fine GF, Cavanagh LM, Afonja A, Binions R (2010) Metal oxide semi-conductor gas sensors in environmental monitoring. *Sensors* 10:5469–5502
- Garde SA (2010) LPG and NH<sub>3</sub> sensing properties of SnO<sub>2</sub> thick film resistors prepared by screen printing technique. *Sens Transducers J* 122(11):128–142
- Hermann K, Witko M, Druzinic R, Chakrabarti A, Tepper B, Elsner M, Gorschlüter A, Kuhlenbeck H, Freund H-J (1999) Properties and identification of oxygen sites at the V<sub>2</sub>O<sub>5</sub> (010) surface: theoretical cluster studies and photoemission experiments. *J Electron Spectrosc Relat Phenom* 98–99:245–256
- Iftikhar AM, Massar KA (2017) Improving NO<sub>2</sub> sensitivity of porous silicon by functionalization its surface with copper as catalyst. *Sci Int (Lahore)* 29(6):1237–1240
- Isam IM, Shahad SH, Fuad IT (2015) Sensing behavior of CuO-doped ZnO/PS nanoparticles. *Mater Lett* 157:57–62
- Johansson D (2011) VO<sub>2</sub> films as active infrared shutters, Ph.D. Thesis, University of Linköping, p 67
- Josephine RL, Suja S, Raj D (2015) Application of renewable energy constant current source in the formation of uniform surfaced. *ARPN J Eng Appl Sci* 10(8):3713–3716
- Kaid MA (2006) Characterization of electrochromic vanadium pentoxide thin films prepared by spray pyrolysis. *Egypt J Solids* 29(2):273–291
- Margoni MM, Ramamurthi K, Mathuri S, Manimozhi T, Rameshbabu R, Sethuraman K (2015) Studies on pure and fluorine doped vanadium pentoxide thin films deposited by spray pyrolysis technique. *Int J ChemTech Res* 7(3):1072–1078
- Mousavi BM, Kompany A (2012) Study of structural, electrical and optical properties of nano-structured vanadium oxide thin films by spray pyrolysis method: effect of solution concentration, 4th international conference on nanostructures (ICNS4) (200), pp 12–14
- Mrigal MEJA, Addou M, Khannyra S (2015) V<sub>2</sub>O<sub>5</sub> thin layers elaborated by spray pyrolysis deposition time effect on the structural, optical and electrochemical properties. *Int J Adv Res Phys Sci* 2(6):24–29
- Ozutok F, Bilgin K, Erturk V (2012) Growth, electrical, and optical study of ZnS: Mn thin films. *Acta Phys Pol A* 121(1):221–223
- Pan A, Zhang J-G, Nie Z, Cao G, Arey BW, Li G, Liang S, Liu J (2010) Facile synthesized nanorod structured vanadium pentoxide for high-rate lithium batteries. *J Mater Chem* 20(41):9193–9199
- Phanichphant S (2014) Semiconductor metal oxides as hydrogen gas sensors. *Proc Eng* 87:795–802
- Prameela C, Anjaiah M, Murthy KK, Srinivasarao K (2013) Structural, optical and electrical properties of (V<sub>2</sub>O<sub>5</sub>)<sub>1-x</sub>-(MoO<sub>3</sub>)<sub>x</sub> thin films. *Indian J Pure Appl Phys* 51(8):563–568
- Prociow E, Zielinski M, Sieradzka K (2011) Electrical and optical study of transparent V-based oxide semiconductors prepared by magnetron sputtering under different conditions. *Radio-Engineering* 20(1):204–208
- Rivoalen L, Revcolevschi A, Livage J, Collongues R (1976) Amorphous vanadium pentoxide. *J Non-Cryst Solids* 21(2):171–179
- Shevchuk VN, Usatenko YN, Demchenko PY, Antonyak OT, Serkiz RY (2011) Nano- and micro-size V<sub>2</sub>O<sub>5</sub> structures. *Chem Met Alloy* 4:67–71
- Shrividhya T, Mahalingam T, Ravi G (2015) Physical property exploration of highly oriented V<sub>2</sub>O<sub>5</sub> thin films prepared by electron beam evaporation. *New J Chem* 39(12):9471–9479
- Sieradzka K (2011) Structural and optical properties of vanadium oxides prepared by microwave-assisted reactive magnetron sputtering. *Opt Appl* XLI(2):1–7
- Sujitno T, Sudjatomoko S (2011) The influence of platinum dopant on the characteristics of SnO<sub>2</sub> thin film for gas sensor application. *Atom Indones* 32(2):65–79
- Tashtoush NM, Kasasbeh O (2013) Optical properties of vanadium pentoxide thin films prepared by thermal evaporation method. *Jordan J Pharm Sci* 6(1):7–15

- van der Drift A (1967) Evolutionary selection: a principle governing growth orientation in vapour-deposited layers. *Philips Res Rep* 22:267–288
- Vijayakumar Y, Reddy KN, Moholkar AV (2015) Influence of the substrate temperature on the structural, optical and thermoelectric properties of sprayed  $V_2O_5$  thin films. *Mater Technol* 49(3):371–376
- Wang C, Yin L, Zhang L, Xiang D, Gao R (2010) Metal oxide gas sensors: sensitivity and influencing factors. *Sensors* 10:2088–2106